COHERENCE PROPERTIES OF POLARIZED RADIATION IN WEAK MAGNETIC FIELDS

LEWIS L. HOUSE

High Altitude Observatory, National Center for Atmospheric Research Boulder, Colorado, U.S.A.*

Abstract. The scattering of radiation in the presence of weak magnetic fields can give rise to coherence or interference phenomena that will profoundly affect the frequency, geometric, and polarization properties of the scattering event. In this paper we discuss and illustrate some of the features of the coherence phenomena associated with the scattering redistribution for the normal Zeeman triplet. The frequency dependent as well as the frequency independent scattering function is considered in a linear polarization basis. In addition we illustrate some properties of this redistribution function in the Stokes representation. Since the primary purpose of this paper is to demonstrate the nature of some of the properties of the coherence problems, that might be important in the interpretation of magnetic fields from polarization measurements of scattered radiation, it has been necessary in this initial work to neglect several features of the problem which are noted in the paper and are currently under investigation.

1. Introduction

To deduce the strength and direction of magnetic fields in solar prominences from the measurement of polarization requires that one utilize the scattering theory of radiation to interpret the measurement. In particular, for scatterings that take place in the presence of weak magnetic fields one must include in the scattering theory the quantum electrodynamic effects of coherence or correlation. This phenomena arises when the sublevels of the scattering atoms are weakly removed from degeneracy by the magnetic field and it manifests itself in the fact that a coherence or correlation is produced between the incoming and outgoing properties of the radiation field – that is, there is a coherence produced between the incoming and outgoing frequencies, directions of propagation, and polarizations. Thus if the scattering takes place under conditions that produce coherence, one may not interpret the measurement of polarization in terms of magnetic fields using the standard theory of scattering in normal Zeeman patterns. Hyder (1964), as well as others, have pointed this fact out in relation to scattering in prominences. This coherence phenomena was discussed in relation to laboratory experiments by Hanle (1924) after whom the effect is named.

In a series of papers (House 1970a, b, c) a general formulation has been given for the scattering redistribution function accounting for the frequency, geometric, and polarization properties of the event, applicable to any dipole transition. Beginning with the work of Weisskopf (1931), it has been possible to cast the general scattering redistribution function into a form that conveniently illustrates how the scattering in the standard Zeeman pattern is modified due to the coherence effects. The theory has been formulated in three polarization basis sets: linear, circular, and in terms of

* The National Center for Atmospheric Research is sponsored by the National Science Foundation.

Howard (ed.), Solar Magnetic Fields, 130–140.

Stokes parameters. A discussion of the coherence problem has also been given recently by Lamb (1970, 1971).

In this paper I should like to show the results of some calculations that illustrate the nature of the coherence phenomena associated with the general scattering function. First, however, let me briefly remind you in somewhat more detail of the origin of the coherence effects.

2. Origin of the Coherence

To see more explicitly how the coherence effects arise let us refer to Figure 1. Here we depict two bound levels of an atom, split into their magnetic sublevels. The components for the ground state are shown a second time so that the difference between the initial and final states of the atom may be more easily seen.

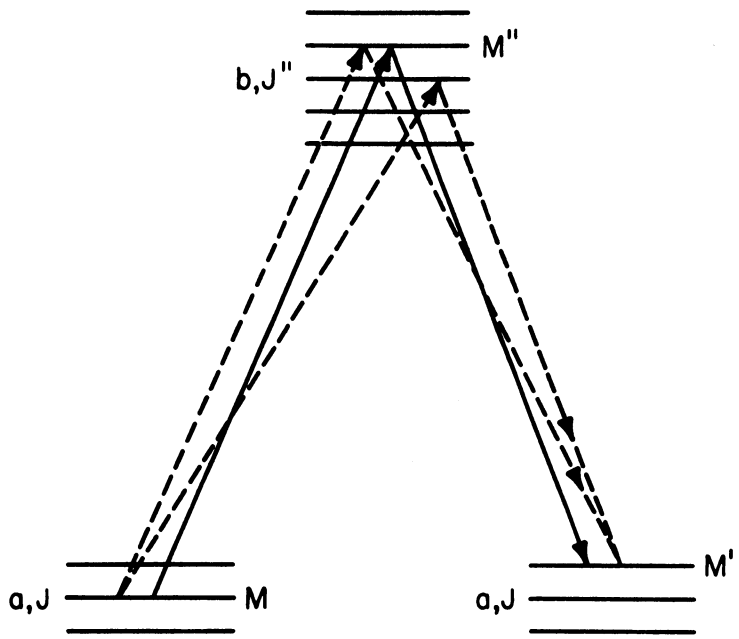

Fig. 1. Schematic energy level diagram showing quantum number designations and typical transitions where coherency effects are not encountered (——) and where coherency does arise (– – – –).

Let us consider two scattering events. First, in the situation where the sublevels are far removed from degeneracy, there is no overlap of the levels, that is, each level is independent. If the excitation raises the atom to an excited state sublevel M'', the subsequent decay occurs from this level back to the ground state (sublevel M') – neglecting collisions and interlocking with other levels. However, if the sublevels are not far removed from degeneracy, that is, if their separation is comparable to or less than the level width, then, quantum mechanically these levels are virtually indistinguishable. In computing the scattering amplitude one must therefore sum over all the

intermediate sublevels that could be excited by the incident radiation and could decay back to the ground state. This must be done, of course, accounting for the angular momentum selection rules. Because the summation over intermediate levels is carried out before one squares the amplitude to obtain the intensity of the scattered radiation, cross terms can arise and these in fact produce the coherence or correlation. After taking the modulus squared, sums over initial as well as final substates must also be carried out. In this situation of weak fields, the scattering event cannot be considered

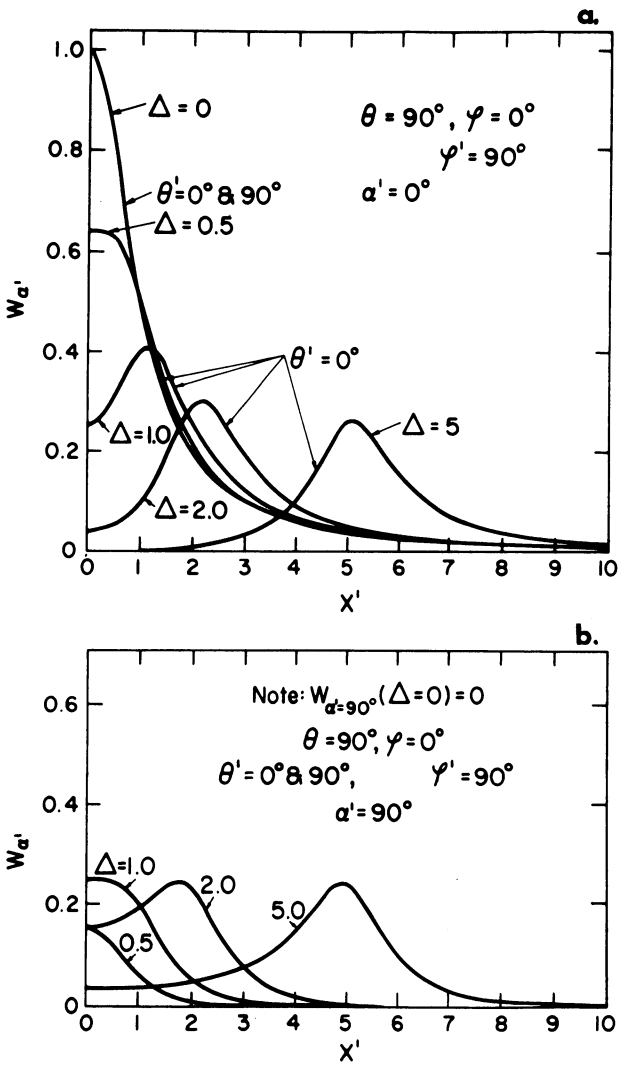

Fig. 2. Emission probability as a function of frequency for various values of Δ and for $\theta' = 0°$ and 90°; (a) applies for the polarization angle $\alpha' = 0°$ while (b) applies for the angle $\alpha' = 90°$. Note in (a) the emission probability is independent of Δ for the observing direction $\theta' = 90°$ and it is, in fact, given by the curve labeled $\Delta = 0$.

https://doi.org/10.1017/S0074180900022488 Published online by Cambridge University Press

as a sequence of an absorption followed by an emission; it must be treated as a single event. Rather than discuss or illustrate the complicated equations that arise in this process, let me proceed to illustrate some calculations based upon the general scattering redistribution function.

3. The Scattering Redistribution Function in Linear Polarization

For the illustrations that I have selected, I have chosen the atomic transition $J=0$ to $J''=1$, that is the normal Zeeman triplet. In addition, for simplicity we will assume that the incident radiation field is unpolarized and independent of frequency over the width of the redistribution function. We shall treat the problem in a linear polarization basis, treat only single scatterings, and neglect collisions.

(a) *Frequency Dependent* – With these assumptions in mind, the next figure, Figure 2, shows a sample computation of the frequency dependent redistribution function where the magnitude of the function is on an arbitrary vertical scale and the horizontal axis is frequency measured from line center in units of the natural width. The splitting due to the magnetic field which is specified by Δ, is also measured in units of the natural width. (I might say for reference that for a transition having an Einstein transition probability of $10^8\ s^{-1}$, the value of $\Delta=1$, corresponds to a magnetic field of about 6G.) The incident radiation is taken to be perpendicular to the magnetic field, $\theta=90°$, and in part (a) of the slide, we have the redistribution function as seen in one state of linear polarization specified by the polarization angle $\alpha'=0°$ while in part (b) we have the orthogonal state of polarization, $\alpha'=90°$. The angle θ' is measured between the direction of the magnetic field and the line of sight. In part (a) of this figure we see that for viewing the radiation along the direction of the field lines, i.e. $\theta'=0°$, the redistribution function gradually decreases in amplitude and shifts outward as the field strength increases. However, if we look perpendicular to the field, the one function labeled $\Delta=0$ is in fact independent of the field strength. Thus in this state of polarization, as the field strength increases, it is only when we look along the magnetic field that the components shift outward. In the orthogonal state of polarization, as shown in part (b), however, these redistribution functions are obtained for directions both along and perpendicular to the magnetic field.

For the larger values of Δ, the scattering redistribution function is approaching that of the normal Zeeman pattern, for we can see that along the field the components in the two orthogonal states of polarization approach being equivalent which will correctly yield zero linear polarization at the position of the shifted component, i.e. at $x'=\Delta$. Perpendicular to the field, we will have a central unshifted component in one state of polarization and a shifted component in the orthogonal state of polarization, thus giving the usual Zeeman results. This figure therefore illustrates the transition from weak fields toward the normal Zeeman pattern.

The polarization resulting from these scattering functions is better illustrated in the next slide, Figure 3, where we can see the degree of linear polarization as a function of frequency for the scattering functions given on the previous slide. As one can see, for

viewing both along the magnetic field as shown in part (a) and perpendicular to the field as shown in part (b), the degree of polarization at the position of the shifted component, $x' = \Delta$, is very sensitive to the field strength; along the field varying from 100% to 0% as Δ varies from 0 to 5 and perpendicular to the field varying from plus 100% to -70% at $\Delta = 5$.

(b) *Frequency Independent* – Next we illustrate some of the more gross properties of the scattering function that have been obtained by integrating over both incoming and outgoing frequencies: that is, we shall look for a moment at some of the properties of the frequency independent scattering function.

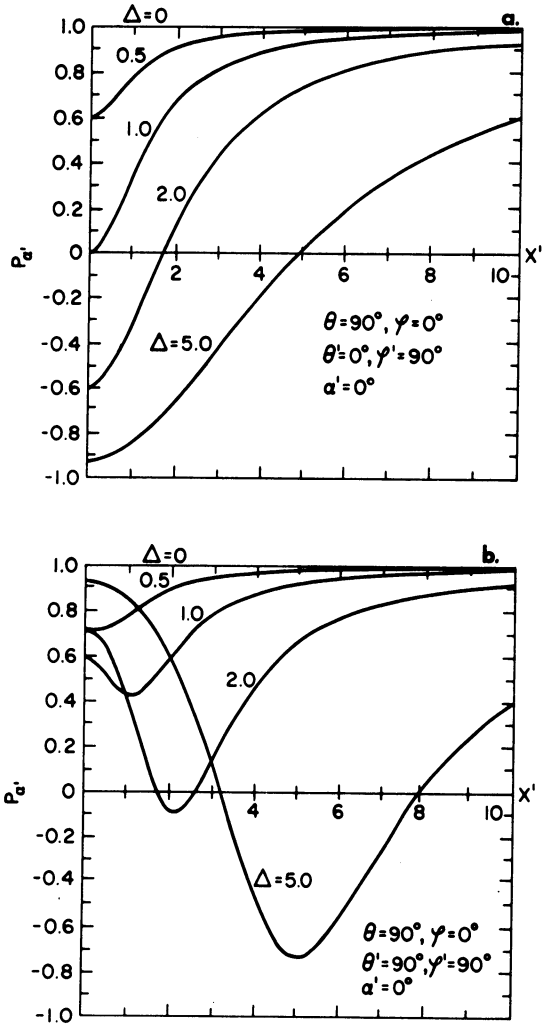

Fig. 3. Degree of polarization for emission probabilities of Figure 2, as a function of frequency curves are given for various values of Δ and for two viewing directions (a) $\theta' = 0°$, $\phi' = 90°$ and (b) $\theta' = \phi' = 90°$.

https://doi.org/10.1017/S0074180900022488 Published online by Cambridge University Press

In Figure 4, scattering diagrams show the intensity of the radiation field again for unpolarized radiation that is incident perpendicular to the magnetic field and unpolarized and where the observer looks along the magnetic field. The length of the vector in these diagrams is proportional to the intensity of the radiation scattered into the state of linear polarization at an angle α, where α is measured counter clockwise from the axis projected vertically downward. These calculations, for various values of the field strength as specified by Δ, show the essential features of the Hanle effect. We see at

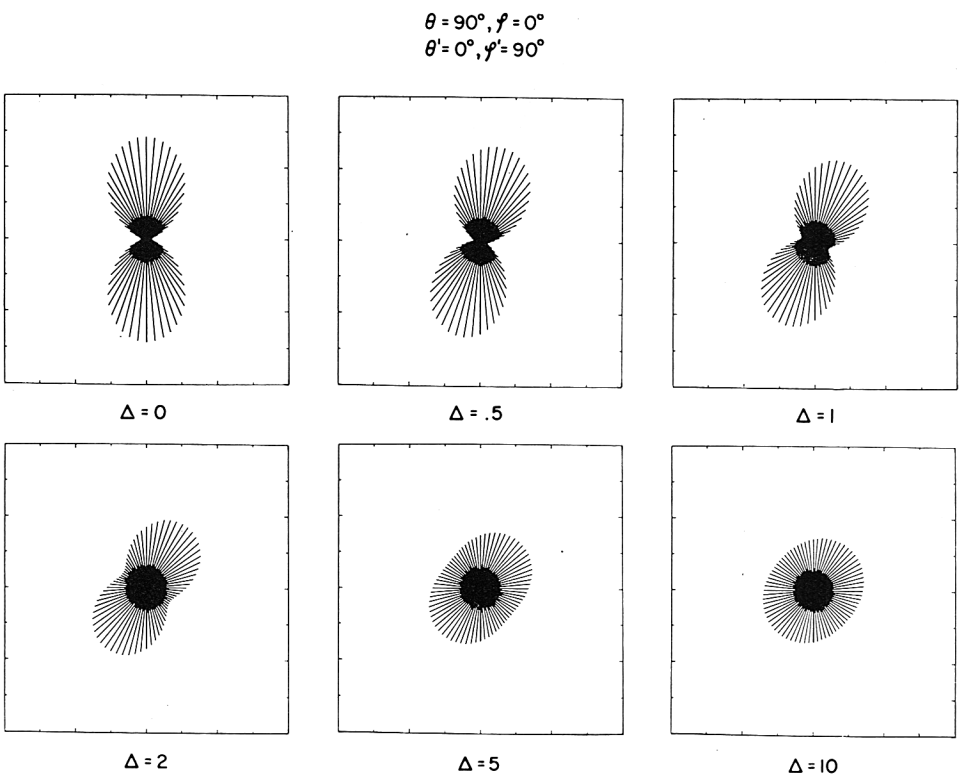

Fig. 4. Frequency independent scattering probability for various values of α'. Vectors indicate magnitude of scattering probability as a function of α' where α' is measured counter-clockwise from the downward vertical direction.

zero magnetic field, we have the usual $\sin^2$ distribution of radiation and a maximum polarization of 100%. As the strength of the field is increased, the angle for the maximum degree of polarization rotates and at the same time, the maximum degree of polarization decreases because the radiation is filling in the direction orthogonal to the direction of maximum intensity. For large values of Δ, we see that unpolarized radiation would be obtained, that is, equal intensities at all polarization angles.

To see how the angle between the magnetic field and the observer influences the polarization, we refer to the next figure, Figure 5. Here I have plotted the maximum

https://doi.org/10.1017/S0074180900022488 Published online by Cambridge University Press

polarization against the angle at which this polarization occurs. The different curves are parameterized by the angle between the observer and the magnetic field, that is, we have θ' varying from along the field, $\theta'=0°$, to $\theta'=90°$, which is perpendicular to the magnetic field. The points distributed along the curves are for the indicated values of the magnetic field strength in terms of Δ. The curve for $\theta'=0°$ shows the maximum polarization which varies from 100% to 0%, as the angle of maximum polarization varies from 0° to 45°. As one alters the viewing angle from along the field to 30°, 60°, and finally to 90° to the field, we see that the range in maximum polarization, as well

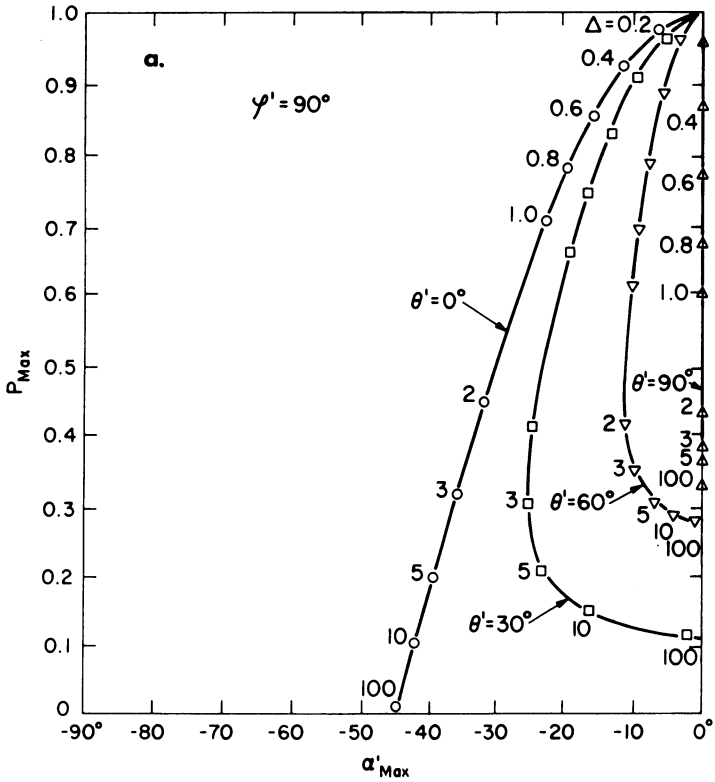

Fig. 5. Degree of maximum polarization versus angle of maximum polarization for various values of θ' and Δ. The different values of Δ are labeled at appropriate positions along the curves.

as the angle of maximum polarization, become somewhat restricted. Thus, if one were to view a single scattering from a point perpendicular to the incident radiation, then, from a measurement of the maximum polarization and the angle of maximum polarization, one could in principle determine the strength of the field as well as the angle between the line of sight and the direction of the field.

Naturally, in the solar atmosphere one does not have such a restricted direction for the incident radiation field, as we have assumed in the previous calculations, because from any single scattering point above the disk, for example in a prominence, one

https://doi.org/10.1017/S0074180900022488 Published online by Cambridge University Press

must consider radiation incident from all angles subtended by the solar disk. The effects of such an integration over the disk of the Sun are shown on the next figure, Figure 6. Here we have plotted the maximum polarization as a function of height above the limb. Part (a) of the figure applies to the situation where the line of sight is

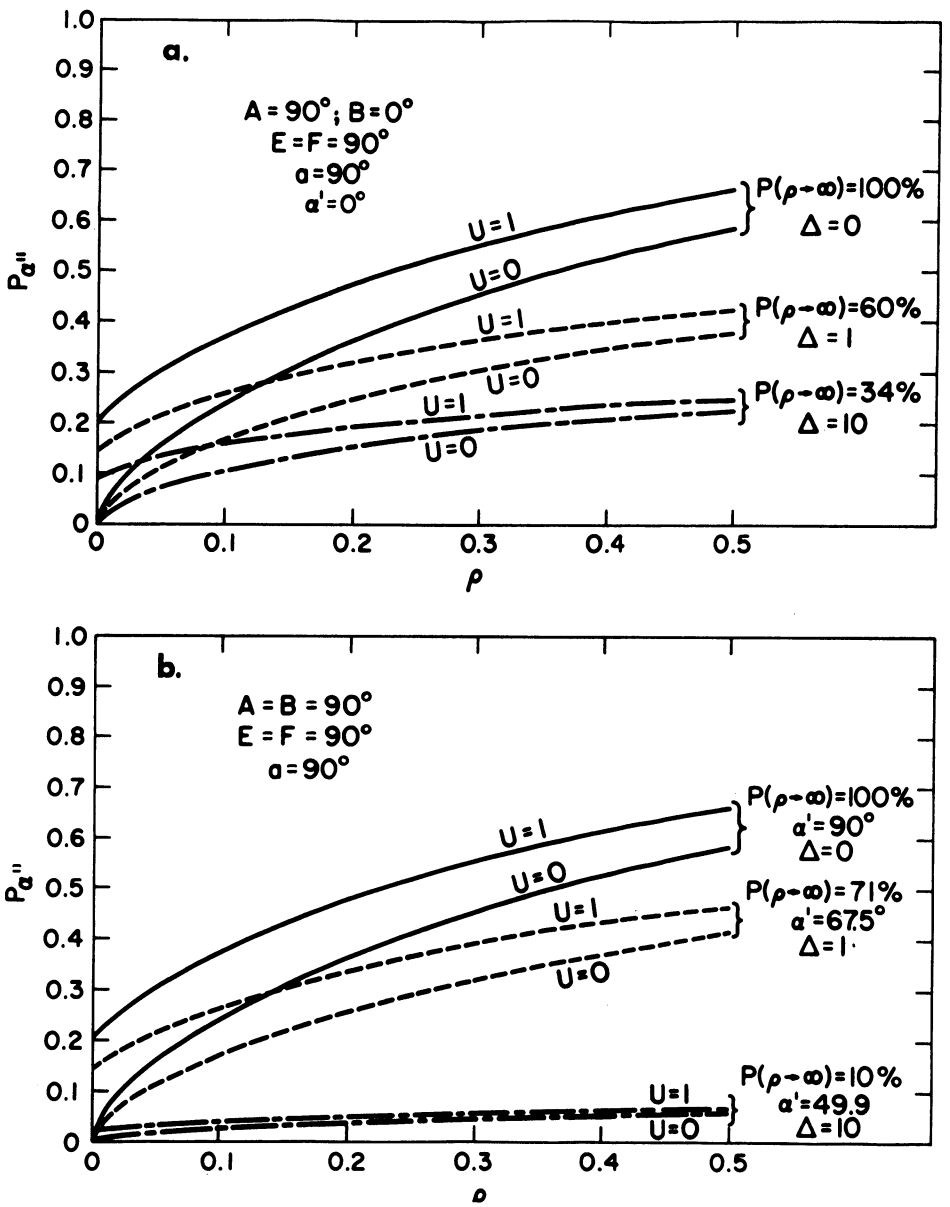

Fig. 6. Degree of polarization as a function of height, ρ, for two values of the limb darkening coefficient ($U = 0$ and 1) and for three values of magnetic field ($\Delta = 0$, 1, and 10). The magnetic field is tangent to the limb and the observer's direction is perpendicular to the field in (a) whereas in (b) the observer's direction is along the field.

https://doi.org/10.1017/S0074180900022488 Published online by Cambridge University Press

perpendicular to the magnetic field and part (b) applies for the observer looking along the direction of the magnetic field. In both cases the line of sight and the magnetic field are tangent to the limb. Curves are given for three values of the strength of the field in terms of Δ and for each Δ, two curves are given, one for a limb darkening coefficient $U=1$ and the other for no limb darkening, or $U=0$. In this figure we see the extent to which the degree of anisotropy as well as the strength and direction of the magnetic field combine to control the degree of linear polarization. The asymptotic limits for the degree of polarization from a point source are given. We note that quite close to the surface of the disk, the polarization can in general vary from about 0 to 20% depending upon the combination of the various parameters.

4. Circular and Stokes Polarization Basis Sets

In the previous calculations a linear basis set for the polarization vector has been used. We may if we wish, however, expand the scattering function in terms of a circular polarization basis set. A series of calculations similar to those just shown in terms of circular polarization have been done. However, rather than show some of these calculations, I would prefer to say something about the formulation of the scattering redistribution function in the Stokes representation.

For a particle, such as a photon having two spin components, a very convenient approach to the Stokes representation is through the quantum mechanical density matrix formulation. In this approach, the fundamental quantum mechanical nature of the Stokes parameters becomes apparent and they are seen to be just the expansion coefficients of the density matrix in terms of the Pauli spin operators or equivalently the projections for the Pauli spin operators in a polarization space. In transforming the scattering redistribution function into the Stokes representation, one subsequently obtains a Mueller matrix for the resonance fluorescence process which includes coherence effects. Thus, the atom can be treated as an 'optical device' that transforms the incident set of Stokes parameters into an outgoing set. The general Mueller matrix is a 4×4 matrix where each element consists of four terms because of the combinations of two independent states of polarization, and each term depending upon the transition may contain up to 19 components in the general expansion; each component depending upon incoming and outgoing frequency, angles of propagation and polarizations, as well as the strength and direction of the magnetic field.

Again we show a sample calculation of the influence of coherency, this time in the Stokes representation.

In Figure 7, we see an illustration of how the Stokes parameters are modified in a single scattering as a function of the strength of the magnetic field. The Stokes parameters are listed for the incoming radiation and for the scattered radiation. In addition, the polarization ellipse as determined by these Stokes parameters is also shown. In this particular case, which is treated as frequency independent, we have chosen an arbitrary state of elliptic polarization for the photon which is incident along the direction of the magnetic field; in this example, the scattering takes place in the

forward direction. (The rotation of the ellipse axis at zero magnetic field, relative to the incident radiation is due to a change in the local coordinate system and should be disregarded at this time.) For increasing magnetic field, the polarization ellipse is seen to rotate and at the same time the scattered photon becomes circularly polarized as indicated by S_3, while the degree of linear polarization, indicated by S_1 and S_2 decreases. This of course must be the case, since in the usual Zeeman theory, only

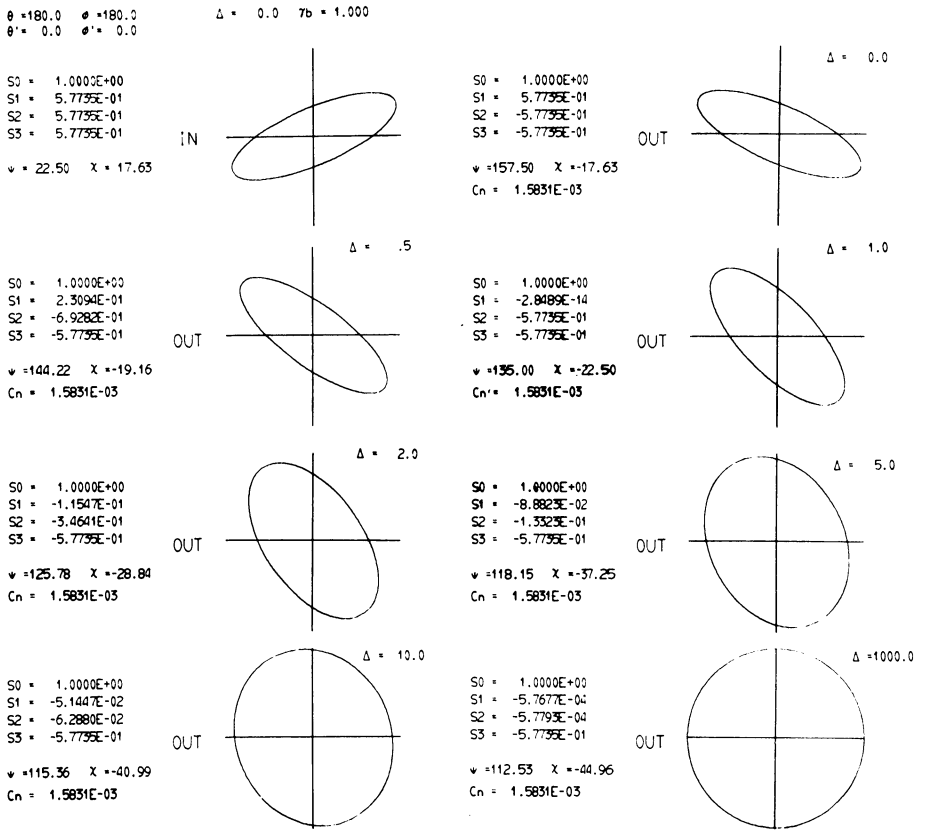

Fig. 7. Stokes parameters and polarization ellipses for a single scattering as a function of Δ. The radiation incident (IN) along the direction of the magnetic field is scattered (OUT) in the forward direction. The four Stokes parameters as well as the parameters defining the polarization ellipse are shown. Rotation between IN and OUT: $\Delta = 0$ is a result of change of coordinate systems and is not to be regarded as real.

circular polarization is observed along the magnetic field if the excitation occurs through circular polarization. This illustration is again meant to point out the sensitivity of the scattering process to weak magnetic fields and how, for example, if one is to use a polarimeter to determine the Stokes parameters of the radiation field scattered by a prominence – the coherence or Hanle effect must be considered in detail.

https://doi.org/10.1017/S0074180900022488 Published online by Cambridge University Press

5. Additional Features of the Scattering Problem

Three other attributes to the scattering problem must be treated before the theory can be applied to the interpretation of observational data, these are – the influence of the Doppler effect, collisions, and multiple scattering. The treatment of the Doppler effect is straight-forward, but because of the coherence features of the problem it requires an excessive amount of space and time even on a computer as large as the CDC-6600. These numerical calculations are however, in progress. Collisions at the present time can be incorporated by increasing the damping width of the states. To include collisions in detail, the statistical equilibrium equations must be treated and since in the radiation part of the problem, the scattering is considered a single event, this leads to difficult problems in including collisions.

Multiple scattering, that is setting up the transfer equation using the general redistribution function, is also complicated because of the coherence or correlation in all of the variables, each of which depends upon the strength and direction of the local magnetic field. Work is currently in progress on this part of the problem where the radiation transport is being done using the Monte Carlo technique. This technique is selected so that a wide range of geometric configurations may be handled. We have already reported some simplified preliminary studies on the influence that multiple scattering and the Hanle effect have upon the depolarization of scattered radiation (House and Cohen, 1969).

References

Hanle, W.: 1924, *Z. Phys.* **29**, 93.
House, L. L.: 1970a, *J. Quart. Spectr. Radiative Transfer.* **10**, 909.
House, L. L.: 1970b, *J. Quart. Spectr. Radiative Transfer.* **10**, 1171.
House, L. L.: 1970c, *J. Quart. Spectr. Radiative Transfer.* in press.
House, L. L. and Cohen, L. C.: 1969, *Astrophys. J.* **157**, 261.
Hyder, C. L.: 1964, *Astrophys. J.* **140**, 817 (For additional references see House, 1970).
Lamb, F. K.: 1970, *Solar Phys.* **12**, 186.
Lamb, F. K.: 1971, this volume, p. 149.
Weisskopf, V.: 1931, *Ann. Phys.* **9**, 23.

Discussion

Brueckner: (1) Did you use in your calculations the assumption of pure scattering?
(2) Are your calculations concentrated on optically thin lines (one scattering event)?

House: As stated in the introduction and conclusions, I treat at this time only a single scattering event. The main purpose of this presentation is to illustrate the properties of the scattering redistribution function. It is necessary to include effects of Doppler broadening, collisions, and multiple scattering before calculation may be compared with observations in prominences.